

Characterization and Activity of Cr, Cu and Ga Modified ZSM-5 for Direct Conversion of Methane to Liquid Hydrocarbons

Nor Aishah Saidina Amin^{1,*}, Didi Dwi Anggoro^{1,2}

¹ Faculty of Chemical and Natural Resources Engineering, Universiti Teknologi Malaysia, 81130 Skudai, Johor, Malaysia;

² Department of Chemical Engineering, University of Diponegoro, 23589 Semarang, Indonesia

[Manuscript received April 02, 2003; revised May 09, 2003]

Abstract: Direct conversion of methane using a metal-loaded ZSM-5 zeolite prepared via acidic ion exchange was investigated to elucidate the roles of metal and acidity in the formation of liquid hydrocarbons. ZSM-5 ($\text{SiO}_2/\text{Al}_2\text{O}_3=30$) was loaded with different metals (Cr, Cu and Ga) according to the acidic ion-exchange method to produce metal-loaded ZSM-5 zeolite catalysts. XRD, NMR, FT-IR and N_2 adsorption analyses indicated that Cr and Ga species managed to occupy the aluminum positions in the ZSM-5 framework. In addition, Cr species were deposited in the pores of the structure. However, Cu oxides were deposited on the surface and in the mesopores of the ZSM-5 zeolite. An acidity study using TPD- NH_3 , FT-IR, and IR-pyridine analyses revealed that the total number of acid sites and the strengths of the Brönsted and Lewis acid sites were significantly different after the acidic ion exchange treatment. Cu loaded HZSM-5 is a potential catalyst for direct conversion of methane to liquid hydrocarbons. The successful production of gasoline via the direct conversion of methane depends on the amount of aluminum in the zeolite framework and the strength of the Brönsted acid sites.

Key words: characterization, activity, modified ZSM-5, methane, direct conversion, liquid hydrocarbons

1. Introduction

Direct catalytic conversion of methane, the principal component of natural gas, to liquid fuels and chemicals of commercial importance remains an intensely sought-after goal. Many researchers have studied the applicability of HZSM-5 and modified ZSM-5 zeolites to the conversion of methane to liquid hydrocarbons [1–9], but the results of their research are still confined to low conversion and selectivity.

The direct partial oxidation of methane to liquid hydrocarbons was reported by Han *et al.* [1,2]. However, methane conversion and liquid hydrocarbon selectivity were too low, and the major product was CO_x (CO and CO_2). They concluded that only Cu, Ni, Zn and Ga-ZSM-5 catalysts could produce liquid hydrocarbons from methane oxidation if the methane or ethane dehydrogenation and olefin oxidation func-

tions of the metals are in balance.

An important intermediate step in the methane and oxygen reaction to produce liquid fuels is the formation of ethylene. Ethylene is then converted to benzene or liquid hydrocarbons over the zeolite support through acid catalyzed oligomerization and cyclization reactions [4–8]. For ethylene oligomerization over ZSM-5, both Brönsted and Lewis acid sites were observed to be active, although Lewis sites have a small advantage in suppressing coke formation [9]. The strong Brönsted acid sites eliminated coke or aromatic formation and allowed only oligomerization to proceed [9]. The amount of framework aluminum is related to the number and strength of the Brönsted acid sites [10,11], an important criteria in ethylene conversion to liquid hydrocarbons [11].

In another study, Pak *et al.* [12] reported a reaction of methane with oxygen that led to a high liquid

* Corresponding author. Tel: 607-5535588; Fax: 607-5581463; Email address: r-naishah@utm.my

hydrocarbon yield (80%) using a two-reactor and recycle system. Unfortunately, this process needed two reactors and many separators to separate the desired products from the diluted product streams.

The reactions of ethane and propane have also been extensively investigated using the ZSM-5 zeolite. For example, Hamid *et al.* [13] studied propane aromatization using modified ZSM-5 zeolites loaded with gallium and prepared by the acidic ion exchange method. In their work, gallium was observed to be distributed on the catalyst surface, in the pores and, more importantly, Ga occupied the aluminum positions in the framework of ZSM-5. Eventually, maximum activity and aromatics selectivity were observed for samples with the highest non-framework dispersed gallium species concentration, which was associated with zeolite Brønsted acidic sites as bifunctional dual sites.

From the previous literature [1,2,6], metal HZSM-5 catalysts were found to encourage:

- (a) the oxidation of methane to methyl species
- (b) the dehydrogenation of paraffins gas hydrocarbons to olefin forms and the dehydrogenation of alicyclic liquid hydrocarbons to aromatic form
- (c) the oligomerization of ethylene and propylene to oligomers (C_5^+).

In this work, the ZSM-5 zeolite was modified by loading it with Cr and Cu from the first-row transition group and with Ga using the acidic ion-exchange method. Our hypothesis is that the activity of the HZSM-5 zeolite catalyst could be increased by the addition of metal ions into the framework. It is predicted that the positions of the metals could increase the activity of the catalyst.

The purpose of this study is to develop, characterize and test the performance of modified ZSM-5 zeolites for the conversion of methane to liquid hydrocarbons. Cr and Cu were chosen for their roles as oxidation and dehydrogenation agents, respectively. Ga, in light of the work carried out by Hamid *et al.* [13], was investigated for its role as an aromatization agent in the conversion of methane to liquid hydrocarbons. The characterization studies were conducted using X-ray diffraction, fourier transfer infra red, ^{29}Si magic angle spinning (MAS), nuclear magnetic resonance (NMR), nitrogen adsorption, ammonia-temperature programmed desorption (NH_3 -TPD) and IR-pyridine. From this study, the roles of metal and acidity in the conversion of methane are determined.

2. Experimental

2.1. Catalysts preparation

ZSM-5 zeolite with a $\text{SiO}_2/\text{Al}_2\text{O}_3$ mole ratio of 30 was supplied by Zeolyst International Co., Ltd., Netherlands. The surface area of the zeolite was $400 \text{ m}^2/\text{g}$. The zeolite was modified by loading it with Cr, Cu or Ga according to the acidic ion exchange method [13].

A known quantity of both metal nitrate solution (molarity=1 M) and the ZSM-5 powder were stirred at a constant pH of about 2. Next, the mixture was refluxed for four hours at 80°C before being washed with distilled water and dried overnight in an oven at 150°C . The metal-loaded ZSM-5 catalysts were then calcined in air at 500°C for five hours.

2.2. Characterization

The characterizations of these catalysts were performed using XRD, FT-IR, ^{29}Si -MAS-NMR, nitrogen adsorption technique (NA), NH_3 -TPD and IR-pyridine. XRD, FT-IR and ^{29}Si -MAS-NMR were employed to determine the zeolite structure and framework Si/Al ratio. Nitrogen adsorption data were pertinent to the zeolite morphology, while NH_3 -TPD and IR-pyridine provided the acidity of catalyst samples.

XRD measurements were performed using a Philips 1840 with Cu K_α radiation, $\lambda=0.154056 \text{ nm}$ at 40 kV and 30 mA in the range of $2\theta=2^\circ$ to 60° at a scanning speed of 4° per minute and a vertical goniometer at room temperature. Samples were saturated over a concentrated NH_4Cl solution in a desiccator to ensure complete dehydration before the pattern was recorded because this could affect the lattice parameter. The powder was ground before being mounted on a glass slide.

^{29}Si MAS-NMR spectra were obtained using a Bruker CXP-300 spectrometer. 90° -pulses were applied at 59.63 MHz and 5 s intervals. No dipolar-decoupling, and thus no cross-polarization, was applied. For the ZSM-5 sample, 18350 FID's were accumulated in 2K data points. The chemical shift was measured with respect to tetramethylsilane and calculated with hexamethyltrisiloxane (-9.8 ppm) as an external reference.

The mid infrared spectra ($1500\text{--}400 \text{ cm}^{-1}$) were recorded on a Shimadzu FT-IR 8000 series using the KBr pellet technique. Thin wafers 13 mm in diameter were made by pressing approximately 10 mg of

fine zeolite powder under 5 tons of pressure for 15 seconds. The thin wafer was placed in a ring-type sample holder and transferred into the IR cell equipped with a CaF₂ window. The IR cell containing the zeolite wafer was attached to the vacuum system (1×10^{-8} mbar pressure). An infrared spectrum for these spectra was recorded on a Shimadzu FT-IR 8000.

The nitrogen adsorption isotherms were obtained at liquid nitrogen temperature using a Sorptomatic 1900 instrument from Fisons Instruments that used a static volumetric technique. The instrument was home-modified by adding two pressure gauges working in the range 0–130 Pa and 0–13 kPa in order to more accurately measure the low-pressure values. The analysis was controlled by microcomputer processing using the MILES-200 and the MILEADP programs for computations.

Infrared spectrums for the hydroxyl group and pyridine adsorption were also recorded on a Shimadzu FT-IR 8000. Thin wafers 13 mm in diameter were made by pressing approximately 10 mg of fine zeolite powder under five tons of pressure for seconds. The thin wafer was placed in a ring-type sample holder and transferred into the IR cell equipped with a CaF₂ window. The IR cell containing the zeolite wafer was placed in the vacuum system (1×10^{-8} mbar pressure).

For hydroxyl group analysis, every zeolite sample was dehydrated at 400 °C for five hours in a vacuum system. The infrared spectra of these samples were recorded at room temperature. Pyridine adsorption was performed at room temperature for the dehydrated sample in a vacuum system. The desorption of pyridine at 150 and 400 °C for two hours was performed in a vacuum system. An IR spectrum was acquired in the absorbance mode at 25 °C with wave numbers between 4000–1300 cm⁻¹ and 2 cm⁻¹ resolution. The infrared spectra of these samples were recorded at room temperature for the analysis of Brønsted and Lewis acid sites with wave numbers between 1700–1400 cm⁻¹.

2.3. Catalyst testing

The performance of the catalysts was tested for methane conversion to liquid hydrocarbons (LHC) via a single step reaction in a fixed-bed micro reactor [6]. Methane with 99.9% purity was reacted with compressed air at atmospheric pressure, 800 °C, F/W of 10440 ml/(g·h) and 9%O₂ (CH₄:O₂=10:1). The reactor was first preheated at 800 °C under a 100 ml/min nitrogen stream for two hours to activate the catalyst.

The reaction products were separated into liquid and gas fractions through an ice-trap.

The methane and liquid hydrocarbon products were analyzed by gas chromatography (GC). GC analyses were carried out using a perkin elmer auto system gas chromatograph equipped with a flame ionization detector (FID) and a hewlett packed-1 (HP-1) capillary column (12 m×0.2 mm×0.33 μm film thickness).

3. Results and discussion

3.1. Structure, framework aluminum and morphology of catalysts

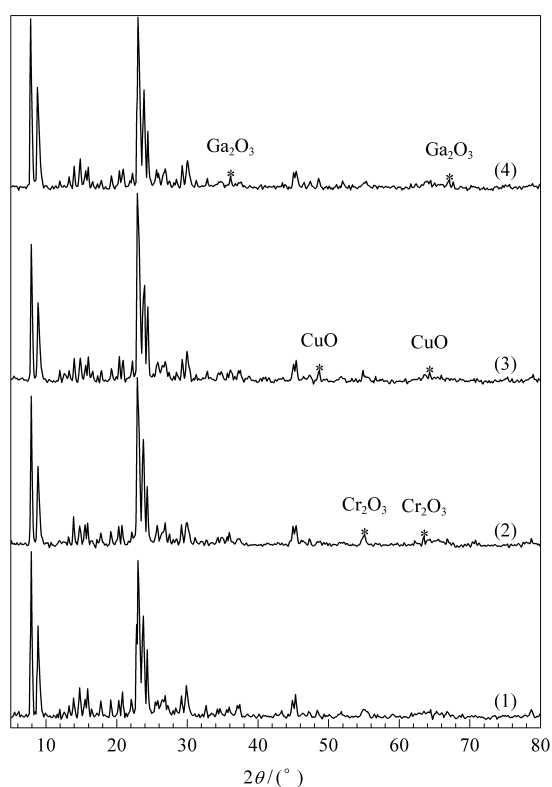
Most of the structural information about ZSM-5 was obtained from X-ray diffraction (XRD). However, XRD is not capable of distinguishing between Si and Al because of their almost equal X-ray scattering properties. Solid-state high-resolution NMR became available with the introduction of superconducting high-field magnets in combination with the magic angle spinning (MAS) technique. Infrared spectroscopy can provide information about the structure of zeolite and the acidic properties.

X-ray diffraction provides information about the unit cell parameters and the crystallinity of the zeolites, as shown in Table 1 based on the XRD diffractograms (Figure 1). The diffractograms revealed that there is no change in the ZSM-5 and metal-loaded ZSM-5 crystalline structure after the acidic ion-exchange modification treatment. The peaks at 2θ values of 24.4° and 29.2° are single peaks for ZSM-5 and metal-loaded ZSM-5 samples, indicating that the structure of the samples did not change from orthorhombic to monoclinic after the modification. The XRD diffractograms also illustrated peaks characteristic of Cr₂O₃, CuO and Ga₂O₃ crystalline on the respective samples, indicating that metal species were distributed on the zeolite surfaces.

The crystallinity of the zeolite can be calculated from the diffractograms. The crystallinity of the zeolite is expressed as the percentage of crystallinity using the intensity of the main peak at $2\theta=22.5^\circ\text{--}24.4^\circ$ in the XRD pattern. Accordingly, the crystallinities of ZSM-5, Cr-ZSM-5, Cu-ZSM-5 and Ga-ZSM-5 are 100, 94, 97 and 99, respectively. The results indicated that the crystallinity of the metal-loaded ZSM-5 did not significantly change in an acidic ion exchange environment. Hence, no change in the ZSM-5 and metal-loaded ZSM-5 crystalline structures were observed.

Table 1. Lattice cell and crystallinity of zeolites from XRD analysis

Sample	Lattice cell				Crystallinity (%)
	a/nm	b/nm	c/nm	V _{uc} /nm ³	
ZSM-5	2.0071	1.9890	1.2746	5.0884	100
Cr-ZSM-5	2.0037	1.9884	1.2729	5.0714	94
Cu-ZSM-5	2.0048	1.9912	1.2737	5.0846	97
Ga-ZSM-5	1.9784	1.9822	1.2626	4.9514	99

**Figure 1. X-ray diffractogram**
(1) ZSM-5, (2) Cr-ZSM-5, (3) Cu-ZSM-5, (4) Ga-ZSM-5

The results in Table 1 indicate that modification of the ZSM-5 with metal had affected the unit cell parameter and volume unit cells. The data shows that the lattice cell parameter and the unit cell volumes (V_{uc}) of the ZSM-5, Cr and Cu loaded ZSM-5 remained the same after the acidic ion exchange treatment. This suggests that the amount of framework aluminum remained intact even after the acidic treatment. However, the lattice cell parameter and the unit cell volume (V_{uc}) for Ga-ZSM-5 decreased. The decrease is a sign that gallium atoms probably occupied the aluminum positions in the framework.

Structural information about the catalyst was obtained with ²⁹Si MAS-NMR. In zeolites, the SiO₄ tetrahedra are connected with 0–4 AlO₄ tetrahedra (Si(OAl)_n, n=0–4) resulting in five distinct ²⁹Si sig-

nals. The framework Si/Al ratio can then simply be calculated from Equation (1) [14]:

$$\frac{\text{Si}}{\text{Al}} = \frac{N_{\text{Si}}}{N_{\text{Al}}} = \frac{\sum_{n=0}^4 I_{\text{Si}}(n\text{Al})}{\sum_{n=0}^4 0.25 \cdot n \cdot I_{\text{Si}}(n\text{Al})} \quad (1)$$

The Si/Al ratio of the metal-loaded ZSM-5 zeolite catalyst samples compared to the parent ZSM-5 is summarized in Table 2. The Si/Al ratios of ZSM-5 and Cu-ZSM-5 are almost similar at 62 and 55, respectively. The similarity implies that probably only a very small number of copper atoms managed to displace aluminum in the zeolite framework. Consequently, the framework aluminum per unit cell of Cu-ZSM-5 is similar to ZSM-5 at 1.7 and 1.5, respectively.

Table 2. The Si/Al ratio and framework aluminum of catalysts from NMR analysis

Sample	Integral Q ₀	Integral Q ₁	Si/Al	Framework Al per unit cell*
ZSM-5	62200.36	4319.82	62	1.5
Cr-ZSM-5	92163.14	2395.26	158	0.6
Cu-ZSM-5	98176.99	7688.70	55	1.7
Ga-ZSM-5	66495.02	1552.60	175	0.5

* Si+Al=96 from Al_nSi_{96-n}O₁₉₂ [15]

Conversely, the Si/Al ratios of Cr-ZSM-5 and Ga-ZSM-5 (158 and 175, respectively) are significantly higher than ZSM-5. The results seem to suggest that more chromium and gallium ions occupied the aluminum positions in the zeolite framework. The framework aluminum per unit cell of Cr-ZSM-5 and Ga-ZSM-5 is 0.6 and 0.5, respectively. The Si/Al ratio of Ga-ZSM-5 seems to support the lattice cell analysis mentioned earlier. However, the Si/Al ratio result and the lattice cell analysis did not support one another for Cr-ZSM-5. There may be some other reasons why the Si/Al ratio is high for Cr-ZSM-5 even though its lattice cell parameters and V_{uc} are the same as the parent ZSM-5.

The resolution of the ²⁹Si NMR spectrum for ZSM-5 drastically decreased with increasing Al content. The Si/Al ratios for the ZSM-5 and metal-loaded ZSM-5 are between 55 and 175. These ratios suggest that only (SiO)₄-Si-(OAl)₀ and (SiO)₃-Si-(OAl)₁ configurations are present. In each unit cell of 96 tetrahedral sites there are only about four Al atoms [16]. The spectra of all samples showed Si(OAl)₀ and Si(OAl)₁ resonances at about –114 and –107 ppm, respectively, indicating that the acidic ion exchange treatment did significantly enhance the resolution.

Figure 2 shows the infrared spectra for ZSM-5 and metal-loaded ZSM-5 samples. The structure sensitive absorption around 1200 and 550 cm^{-1} is of special interest to distinguish the zeolite types [17]. In Table 3 the positions of some characteristic vibration bands are summarized. All samples have vibration bands between 546 and 1223 cm^{-1} . The frequency band at 1099 cm^{-1} is assigned to the asymmetric stretching of framework Si–O–Si or Si–O–Al bonds [18]. The bands of Cr-ZSM-5 and Ga-ZSM-5 demonstrated a significant change in the frequency shift or a reduction in the intensity framework. This indicates that Cr-ZSM-5 and Ga-ZSM-5 catalysts experienced a significant change in the number of those forming framework bonds.

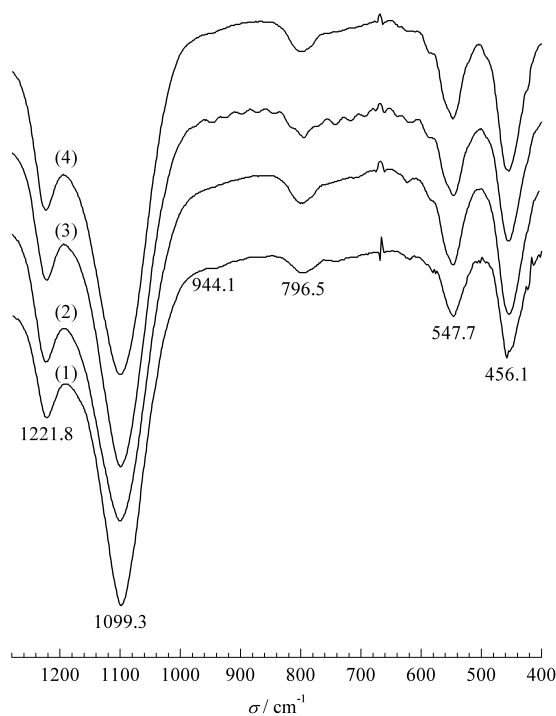


Figure 2. Infrared spectra
(1) ZSM-5, (2) Cr-ZSM-5, (3) Cu-ZSM-5, (4) Ga-ZSM-5

Table 3. Infrared band positions of ZSM-5 and metal loaded ZSM-5

Sample	Wavenumber (cm^{-1})				
	A		S	Double ring	To bending
	External	Internal	External		
ZSM-5	1221.8	1099.3	796.5	547.7	456.1
Cr-ZSM-5	1223.7	1101.3	798.5	546.8	455.2
Cu-ZSM-5	1222.8	1100.3	795.6	545.8	457.1
Ga-ZSM-5	1223.7	1100.3	798.5	545.8	458.1

A—Asymmetric stretch, S—Symmetric stretch

The crystallinity of the samples could be estimated using the IR optical density ratio of the 546 and 454 cm^{-1} bands of zeolite [18]. According to an earlier investigator [18] and our present findings, the optical density ratios of the 546 and 454 cm^{-1} bands of ZSM-5, Cr-ZSM-5, Cu-ZSM-5 and Ga-ZSM-5 are 0.832, 0.829, 0.826 and 0.829, respectively. The ratios suggest that the zeolite framework of all the samples remains intact. This result is consistent with the XRD analysis, which stated that there is no change in the ZSM-5 and metal-loaded ZSM-5 crystalline structure.

The isotherm adsorption of ZSM-5 and metal-loaded ZSM-5 provided the pore distribution data. The presence of a hysteresis loop is associated with capillary condensation, where in the case of zeolite, it indicates the formation of mesopores (secondary pores). The surface area, pore volume and average pore size of the samples are given in Table 4.

From Table 4, the ratio of BET surface area for Cr-ZSM-5 and Ga-ZSM-5 to the ZSM-5 samples does not vary a great deal after metal loading (2% and 4%, respectively). The values obtained are within experimental error. However, the BET surface area ratio of Cu-ZSM-5 to ZSM-5 increases by 8%. This suggests that more copper species form clusters as oxide aggregates on the surface of the ZSM-5 zeolite.

Table 4. The surface area, pore volume and pore size of ZSM-5 and metal ZSM-5

Sample	Surface area (m^2/g)		Pore volume (cm^3/g)		Average pore diameter (nm)
	BET	Micropores (1.7–300 nm)	Single step total	Micropores (1.7–300 nm)	
ZSM-5	361.7	184.2	0.265	0.073	2.93
Cr-ZSM-5	368.9	205.4	0.265	0.087	2.87
Cu-ZSM-5	391.9	198.8	0.277	0.079	2.82
Ga-ZSM-5	374.7	191.5	0.267	0.076	2.85

More chromium and copper species are likely to be attached to the mesopores of the modified zeolite samples, as indicated by the enlargement of the micropore surface areas for Cr-ZSM-5 and Cu-ZSM-5 by

12% and 8%, respectively. The catalyst morphology for Cr-ZSM-5 seems to be interesting because the Si MAS-NMR analysis revealed that Cr species could have replaced aluminium in the framework, and the

NA analysis indicated an increase in the micropore surface area. The micropore surface area of Ga-ZSM-5 only increased by 4% after metal loading. The result seems to support the XRD and Si MAS-NMR data, which suggest that gallium species replaced aluminum in the zeolite framework. The pore volume measured by N₂ adsorption for metal-loaded ZSM-5 only increased 1%–5% after metal loading, which could be considered negligible and within experimental error. The average pore size data categorized all pores as mesopores.

3.2. Acidic properties of zeolite catalysts

For the characterization of zeolite acidity, it is necessary to determine the number and strength of both types of acid sites (Brønsted and Lewis). In this study, infrared spectroscopy of hydroxyl groups, infrared spectroscopy of adsorbed pyridine and temperature programmed desorption of ammonia were the three techniques used to evaluate the acidic properties of ZSM-5 and metal-loaded ZSM-5 catalysts. The total amount of acid sites, as determined by NH₃-TPD, is given in Table 5.

Table 5. The total number of acid sites of ZSM-5 and metal-loaded ZSM-5

Sample	Total number of acid site (mol/kg)
ZSM-5	0.8710
Cr-ZSM-5	0.8145
Cu-ZSM-5	1.0196
Ga-ZSM-5	0.8959

The total amount of acid sites is proportional to the Al content of the framework [19]. The number of acid sites in the Cu-ZSM-5 is the largest at 1.0196 mol/kg. Meanwhile, the number of acid sites in Cr-ZSM-5 and Ga-ZSM-5 is similar to ZSM-5. The number of acid sites in Cu-ZSM-5 increased by 17% as a result of the modification. The increase is probably due to the larger pore volumes of Cu-ZSM-5 that facilitate desorption of ammonia and to the realumination of extra framework aluminium to framework aluminium.

The addition of chromium and gallium by acidic ion exchange did not change the overall number of active acid sites. As mentioned earlier, Ga species have most likely replaced aluminum in the framework. Although there is not enough evidence to suggest that Cr in the Cr-ZSM-5 samples had replaced aluminum in the framework, the similarities in acidity between

Cr-ZSM-5 and ZSM-5 are interesting. From Table 4, the pore volumes for ZSM-5, Cr-ZSM-5 and Ga-ZSM-5 are almost the same, and this probably caused the similar total acidity for all the three samples.

The TPD of NH₃ analysis for the samples is presented in Figure 3. Each data set on the graph has been normalized to distinguish the relative peak areas of weak Brønsted acid from strong Lewis acid sites. For the ZSM-5 and metal-loaded ZSM-5, the NH₃-TPD peaks appeared at ~220 °C and ~430 °C, which may be attributed to the desorption of two types of ammonia species adsorbed on weak acid (mostly Lewis acid) sites and strong acid (mostly Brønsted acid) sites, respectively.

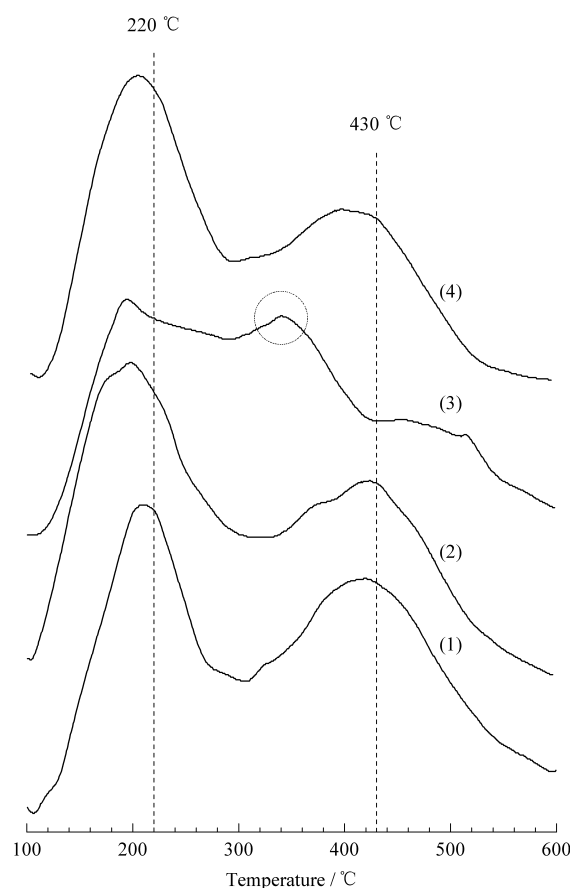


Figure 3. NH₃-spectra TPD

(1) ZSM-5, (2) Cr-ZSM-5, (3) Cu-ZSM-5, (4) Ga-ZSM-5

The loading of metals on ZSM-5 led to reduced intensities of the high-temperature (~430 °C) peaks and a slight downshift of their position. When Cu is loaded on ZSM-5, the high temperature peak disappeared, but a new peak at 370 °C was generated. This indicates that most of the stronger surface Brønsted acid sites vanished, but new medium-strength acid sites emerged.

For a complete characterization of zeolite acidity, it is necessary to determine the nature and concentration of both Brönsted and Lewis acid sites. This is possible by studying the OH vibration infrared spectra and the IR chemisorption of a base such as pyri-

dine. The vibrations (OH) region of the IR spectrum of ZSM-5 contains bands at around 3600 and 3740 cm^{-1} [20,21], as shown in Figure 4. The positions of some characteristic OH vibration bands and integrated band areas are summarized in Table 6.

Table 6. The positions of certain characteristic OH vibration bands and the integrated band area of the catalysts

Sample	Wavenumber (cm^{-1})			Integrated band area		
	Silanol	AL-NF ^a	AL-F ^b	AL-F	AL-NF	Silanol
ZSM-5	3743.6	3659.7	3609.5	88.6	17.7	29.6
Cr-ZSM-5	3744.5	3657.7	3608.6	69.2	39.3	19.2
Cu-ZSM-5	3744.5	3662.6	3607.6	110.8	39.4	21.2
Ga-ZSM-5	3744.5	3662.6	3609.5	69.7	40.6	20.2

a. Aluminum non framework, *b.* Aluminum framework

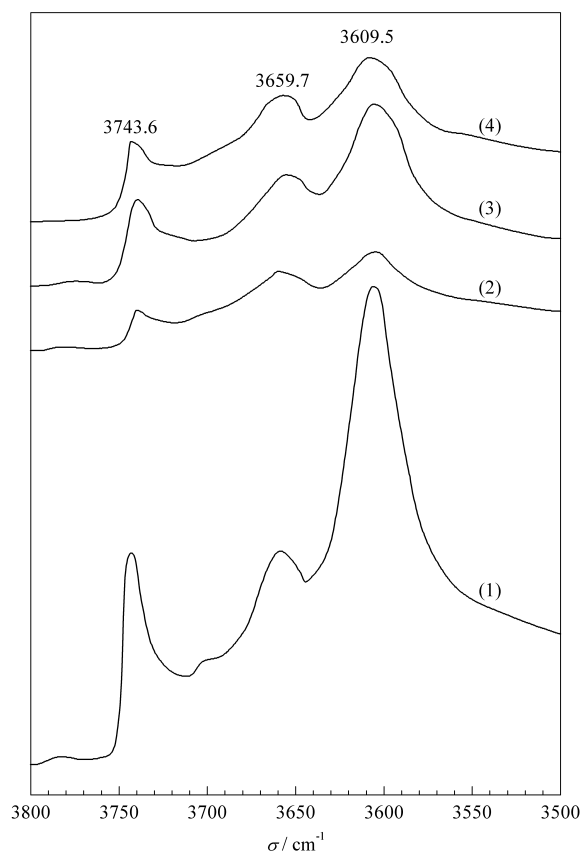


Figure 4. IR spectra in the hydroxyl region of the zeolite samples after dehydration OH at 400 °C, 10^{-5} mbar for 2 h

(1) ZSM-5, (2) Cr-ZSM-5, (3) Cu-ZSM-5, (4) Ga-ZSM-5

The typical stretching vibrational band of the bridging OH groups bonded to tetrahedrally coordinated framework aluminum is located at around 3610 cm^{-1} , as shown in Figure 5(a) [22]. The band at 3660 cm^{-1} is assigned to hydroxyl groups located in non-framework Al sites, while a band at 3649 cm^{-1} is ascribed to OH groups on non-framework aluminum

species, as shown in Figures 5(b) and (c) [23,24]. The band at 3740 cm^{-1} is assigned to terminal silanol groups attached to the framework [21]. This peak is also assigned to the non-acidic silanol groups that are present on the outer surface of the zeolite crystals and at structural defects. Generally, the appearance of this band is an indication of a reduction in crystallinity due to the increasing number of terminal Si-OH groups per unit cell.

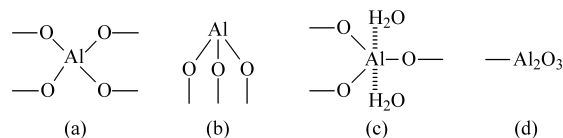


Figure 5. Aluminium position on zeolite [22]

(a) Framework (Tetrahedral), (b) Non-Framework (Octahedral), (c) Non Framework (Pentacoordinated), (d) Extra Framework

The amount of framework aluminum decreased due to the extraction of aluminum from the zeolitic framework to non-framework or into the acidic solution. Table 6 indicates that the framework aluminum (3610 cm^{-1}) area of Cr-ZSM-5 and Ga-ZSM-5 is 69.2 and 69.7 cm^{-1} , respectively. These two areas are smaller than the area of ZSM-5, calculated at 88.6 cm^{-1} . In contrast, the area of the framework aluminum for Cu-ZSM-5 is larger than ZSM-5. These results support earlier data from the Si-MAS-NMR (Table 2) which indicates the framework aluminium per unit cell is 1.7. The value reported is the highest among all the samples. The increase in the framework aluminium area is probably due to the realumination of extra framework aluminum to framework aluminum during the modification [25]. Another reason might be that the Cu-ZSM-5 structure remains intact dur-

ing calcination and is therefore the most stable of all samples [26].

From Table 6, the non-framework aluminum (3660 cm^{-1}) area of all metal-loaded ZSM-5 increased, indicating that the amount of non-framework aluminum increased due to the shift of aluminum in the zeolite framework to its non-framework. In contrast, the silanol (3743.6 cm^{-1}) areas of all metal-loaded ZSM-5 decreased probably due to the extraction of the silanol groups into the acidic solution.

The vibration (OH) region of the IR spectra for ZSM-5 and metal-loaded ZSM-5 subjected to five hours of heating at $800\text{ }^{\circ}\text{C}$ followed by dehydration at $400\text{ }^{\circ}\text{C}$ and 10^{-5} mbar for two hours has bands at around 3600 and 3740 cm^{-1} (Figure 6). ZSM-5 and metal-loaded ZSM-5 samples have no vibration bands at 3610 and 3660 cm^{-1} . ZSM-5 is the one and only sample with a weak vibration band at 3666 cm^{-1} . The results in Figure 6 suggest that the framework and non-framework Al sites are extracted to silanol defect form at $800\text{ }^{\circ}\text{C}$. The large vibration band at 3740 cm^{-1} (Figure 6) indicates this defect.

The IR spectrum of pyridine adsorption on ZSM-5 and metal-loaded ZSM-5 at 150 , 400 and $800\text{ }^{\circ}\text{C}$ is shown in Figures 7(a)-(d). The presence of Brönsted and Lewis acid sites is characterized by the IR spectrum in the region of pyridine ring vibration between 1700 and 1300 cm^{-1} . The assignment of frequencies for pyridine adsorbed on Brönsted and Lewis acid sites is summarized in Table 7.

Table 7. Assignment of frequencies for pyridine adsorbed on Brönsted and Lewis acid sites [22]

Frequency (cm^{-1})	Assignment
1440	Hydrogen-bonded pyridine
1450	Pyridine molecules adsorbed on Lewis acid sites
1490	Hydrogen-bonded pyridine and pyridine molecules adsorbed on Brönsted and Lewis acid sites
1545, 1620–1650	Pyridine molecules adsorbed on Brönsted acid sites, pyridinium ions
1620–1630	Pyridine molecules adsorbed on Lewis acid sites, coordinated pyridine

The IR frequencies of the pyridinium ion and coordinated pyridinium at $150\text{ }^{\circ}\text{C}$, which correspond to the Brönsted and Lewis acidities, respectively, are listed in Table 8. The wavenumber of the Brönsted acidity in Ga-ZSM-5 at 1546 cm^{-1} shifted to 1545 cm^{-1} , indicating that the acidic ion exchange over the gallium solution replaced some of aluminium in the zeolite framework. However, the intensities of the Lewis acidity at 1446 cm^{-1} in Cu-ZSM-5 and Ga-ZSM-5 increased, probably due to the increased amount of non-framework aluminum. The results in Table 6 in-

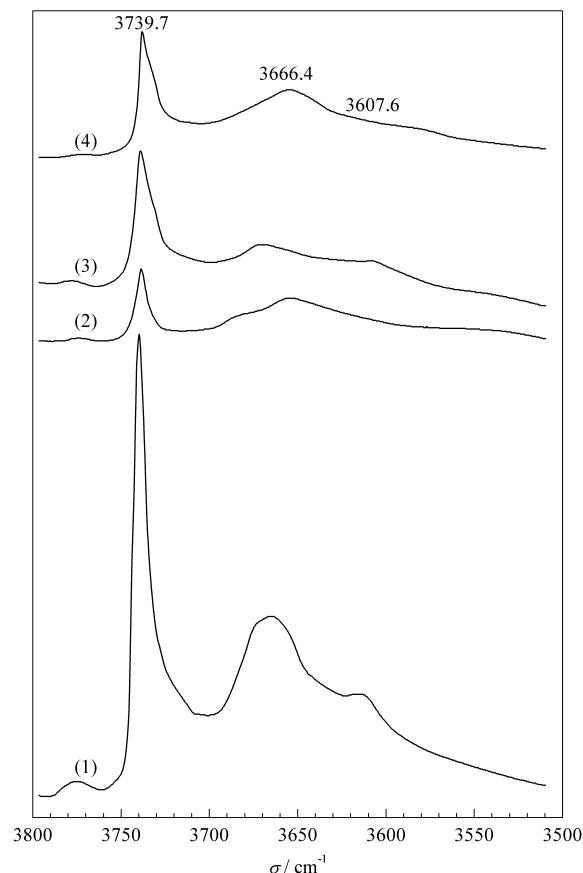


Figure 6. IR spectra in the hydroxyl region of zeolite samples after reaction ($800\text{ }^{\circ}\text{C}$) and dehydration OH at $400\text{ }^{\circ}\text{C}$, 10^{-5} mbar for 2 h

(1) ZSM-5, (2) Cr-ZSM-5, (3) Cu-ZSM-5, (4) Ga-ZSM-5

dicate that the amount of non-framework aluminum (AL-NF) in all metal-loaded ZSM-5 zeolite catalysts increased. The effect of metal-loaded ZSM-5 and the extraction of the framework aluminum in each sample, given as intensity ratio of Brönsted and Lewis acid bands, are clearly shown in Table 8. The bands at wavenumbers of about 3664 and 3608 cm^{-1} still appeared in the spectra, indicating that these bands are not affected by pyridine. This observation suggests that these bands are non-acidic with respect to pyridine.

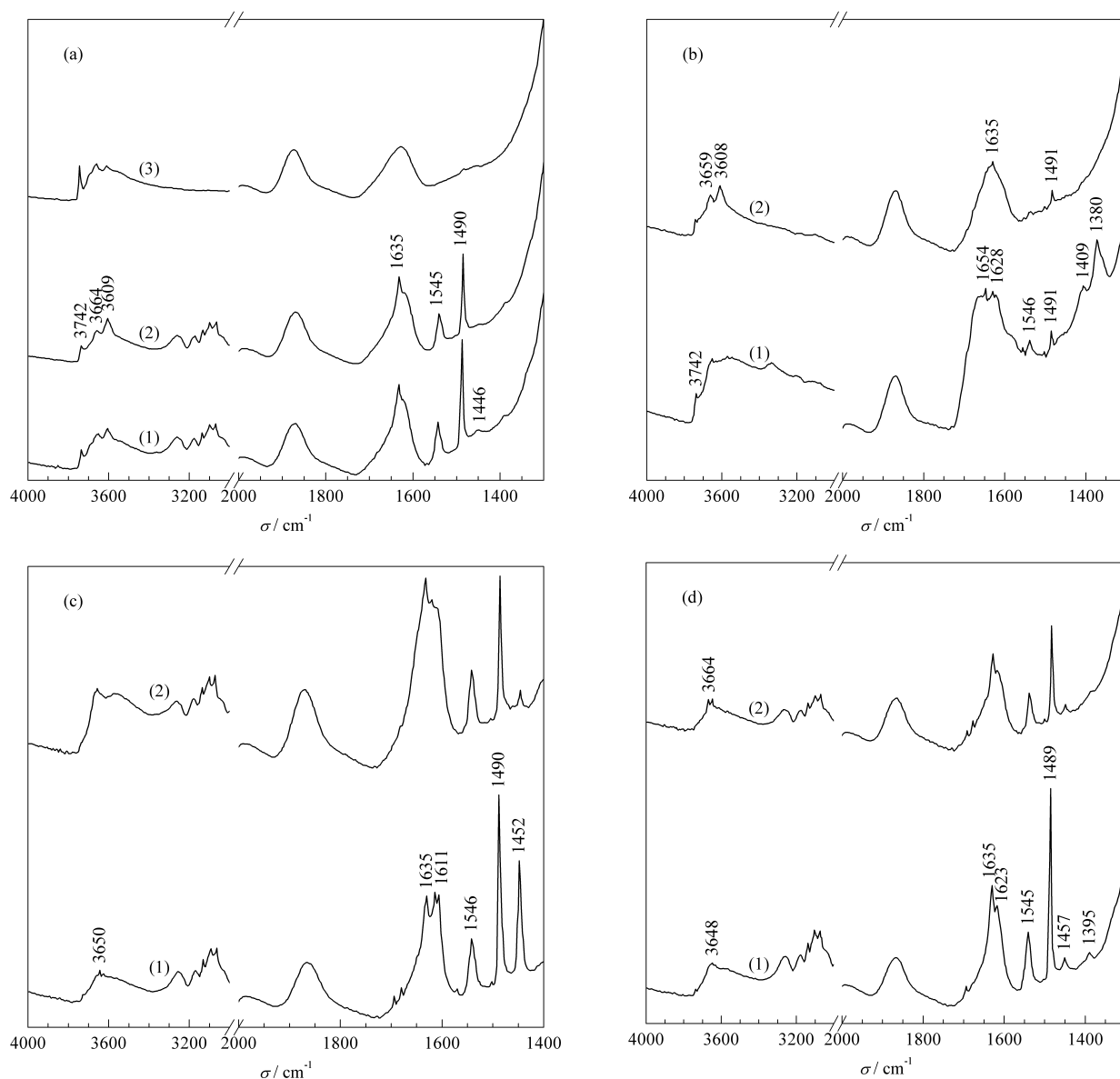


Figure 7. IR spectra in the pyridine vibrational region, after pyridine adsorption and evacuation at different temperatures

(a) ZSM-5, (b) Cr-ZSM-5, (c) Cu-ZSM-5, (d) Ga-ZSM-5; (1) 150 °C, (2) 400 °C, (3) 800 °C

Table 8. Mid-infrared wavenumbers (cm^{-1}) of pyridine and Brönsted/Lewis intensity ratio of ZSM-5 and metal loaded ZSM-5

Sample	Brönsted acidity (cm^{-1})	Brönsted and Lewis acidity (cm^{-1})	Lewis acidity (cm^{-1})	I-B/I-L
ZSM-5	1546	1490	1455	1.48
Cr-ZSM-5	1546	1491	1459	3.22
Cu-ZSM-5	1546	1490	1452	0.91
Ga-ZSM-5	1545	1490	1457	1.65

The amount of Brönsted acidity, Lewis acidity and intensity Brönsted/Lewis (B/L) ratio of pyridine

adsorption on zeolites evacuated at 150 and 400 °C are shown in Table 9. The amount of Brönsted and Lewis acid sites are calculated based on the following [27]:

$$N.\text{Brönsted} = (\text{Integrated of Brönsted Band Area} \times 0.7857) / (3.03 \times 5.92)$$

$$N.\text{Lewis} = (\text{Integrated of Lewis Band Area} \times 0.7857) / (3.8 \times 5.92)$$

The results in Table 9 demonstrate that the amount of Brönsted acidity, Lewis acidity and intensity B/L ratio of pyridine adsorption on the zeolites changed significantly after the zeolites were subjected to pyridine evacuation at temperatures from 150 to 400 °C.

Table 9. The integrated band area of Brönsted and Lewis acid sites and the number of Brönsted and Lewis acid sites in each catalyst

Sample	Temperature evacuation (°C)	I.B.A.B (A/cm ⁻¹)	I.B.A.L (A/cm ⁻¹)	No.B.S. (μ mol/g)	No.L.S. (μ mol/g)	Δ B	Δ L
ZSM-5	150	19.4	13.2	0.852	0.459	7%	12%
	400	18.0	11.6	0.789	0.404		
Cr-ZSM-5	150	18.3	5.7	0.803	0.198	52%	-134%
	400	8.7	13.3	0.383	0.465		
Cu-ZSM-5	150	22.6	24.8	0.989	0.865	4%	46%
	400	21.6	13.3	0.948	0.466		
Ga-ZSM-5	150	24.9	15.1	1.095	0.528	26%	16%
	400	18.4	12.7	0.808	0.445		

I.B.A.B or I.B.A.L=Integrated band area of Brönsted or Lewis

No.B.S or No.L.S=Number of Brönsted sites or Lewis sites

ΔB=(No.B.S at 150 °C–No.B.S at 400 °C)/No.B.S at 150 °C×100%

Δ L=(No.L.S at 150 °C–No.L.S at 400 °C)/No.L.S at 150 °C×100%

The differences between the Brönsted and Lewis acidities and the intensities of the B/L ratio of pyridine adsorption on the zeolites after being evacuated from 150 to 400 °C indicates the strength of Brönsted acidity and Lewis acidity [28,29]. If the difference is large, then the acidity is weak. From Table 9, the acidity strength of the zeolite catalysts can be summarized as follows:

Brönsted acidity strength: Cu-ZSM-5>ZSM-5>Ga-ZSM-5>Cr-ZSM-5

Lewis acidity strength: Cr-ZSM-5>ZSM-5>Ga-ZSM-5>Cu-ZSM-5

3.3. Relation between characterization and performance of catalysts

The conversion of methane and the distribution

of liquid hydrocarbons are based on the peak areas of gas chromatogram and are determined according to:

Conversion of methane=(Area of CH₄ reacted / Area of CH₄ in feed)× 100%

Distribution of products=(Area of *i*/Σ Area of liquid products)×100%

where *i*=C_{5–10} or C₁₁⁺.

The methane conversion and composition of liquid hydrocarbons over ZSM-5 and metal-loaded ZSM-5 are shown in Table 10. The methane conversion of the catalysts can be summarized below:

ZSM-5<Cu-ZSM-5<Ga-ZSM-5<Cr-ZSM-5.

From OH vibration analysis, the results in Table 6 indicate that the integrated silanol band area (3744 cm⁻¹) of the catalysts can be arranged as follows:

ZSM-5>Cu-ZSM-5>Ga-ZSM-5>Cr-ZSM-5

Table 10. The methane conversion and composition of liquid hydrocarbons over ZSM-5 and metal loaded ZSM-5

Sample	CH ₄ conversion (%)	Composition of liquid hydrocarbons product					C ₁₁ ⁺ range	RON
		Gasoline range (C _{5–10})	<i>n</i> -Paraffins	<i>Iso</i> -Paraffins	Olefins	Aromatics		
ZSM-5	10.8	72.4	13.5	22.3	53.4	10.8	27.6	79.2
Cr-ZSM-5	21.0	70.4	9.0	23.0	55.0	13.0	29.5	85.6
Cu-ZSM-5	15.6	80.2	8.0	20.0	57.0	15.0	19.8	87.8
Ga-ZSM-5	18.5	70.1	7.0	17.0	58.0	18.0	26.9	90.2

The integrated silanol band area seems to have affected the methane conversion. The methane conversion decreased if the integrated silanol band area increased. For example, methane conversion of Cr-ZSM-5 is the highest because its silanol area is the lowest. The reduction in silanol area of Cr-ZSM-5 is probably due to chromium being substituted into the silanol groups. Hence, the presence of Cr in the

silanol groups of the zeolite enhanced the methane conversion.

The compositions of the liquid hydrocarbon products can be arranged as follows:

C_{5–10}: Cu-ZSM-5 > ZSM-5 > Cr-ZSM-5 ≈ Ga-ZSM-5

C₁₁⁺: Cr-ZSM-5 > ZSM-5 > Ga-ZSM-5 > Cu-ZSM-5.

The oligomerization and cracking processes depend on the zeolite acidity [30,31]. The self-addition of olefins to form dimmers, trimers, and low polymers is called oligomerization [32]. If the strength of the Brönsted acid sites is strong, the cracking of oligomers is easy. For example, the NH_3 -TPD spectra of Cu-ZSM-5 (Figure 3) indicate that new medium-strength Brönsted acid sites are generated, and this corresponds to the highest percentage of C_{5-10} . In contrast, the strength of the Brönsted acid sites of Ga-ZSM-5 and Cr-ZSM-5 are weaker than ZSM-5, which is linked to the low percentage of C_{5-10} over the two metal-loaded catalysts. Thus, the successful production of gasoline from methane depends on the amount of aluminum in the zeolite framework and the medium-strength Brönsted acid sites.

The results in Table 10 indicate that the *n*-paraffins in the liquid products over the ZSM-5 catalyst are higher than over metal-loaded ZSM-5 catalysts because the ZSM-5 catalyst has no metal content. Metals have dehydrogenation functions to convert paraffins to olefins. Hence, the olefin distribution over metal-loaded ZSM-5 catalysts is higher than over the ZSM-5 catalyst. The Ga-ZSM-5 catalyst has the highest aromatics content in the liquid hydrocarbon products, indicating that the Ga-ZSM-5 catalyst is a potential catalyst for the aromatisation reaction. This result supports the conclusion from previous studies [33–36]. The liquid products over the Cr-ZSM-5 catalyst contain the highest *iso*-paraffins. This could be attributed to its large micropore area probably due to chromium clusters in the zeolite pores that aided the isomerism of the paraffins.

The research octane number (RON) of the liquid hydrocarbons was estimated [37], and the results in Table 10 indicate that the RON of the liquid products obtained over Ga-ZSM-5 is the highest due to its low paraffin and high aromatics content. However, the Cu-ZSM-5 catalyst is a potential catalyst for the direct oxidation of methane to liquid hydrocarbons, because this catalyst yields the highest gasoline composition.

4. Conclusions

The study of structure, framework aluminium, and morphology of metal-loaded ZSM-5 catalysts via acidic ion exchange treatment indicated that the crystalline structures of the samples did not change, and the zeolitic framework remained intact. Also, the

structure of the samples did not change from orthorhombic to monoclinic. Chromium and gallium atoms successfully replaced the aluminium atoms in the zeolite framework by this treatment. Chromium ions were also distributed on the zeolite silanol groups and inside the pores of the zeolite whilst copper ions are deposited on the zeolite surface and the mesopores of ZSM-5.

The study of catalyst acidity indicated the total amount of acid sites of Cu-ZSM-5 is the highest, and its Brönsted acid sites have medium-strength. The framework and non-framework aluminum sites of metal-loaded ZSM-5 were extracted to silanol defect form at the reaction conditions.

From the catalyst testing it can be concluded that Cu loaded HZSM-5 is a potential catalyst for the conversion of methane to liquid hydrocarbons. The existence of silanol groups gave positive impacts on the methane conversion and the successful production of gasoline from methane depends on the amount of aluminium in the zeolite framework and the strength of Brönsted acid sites.

Acknowledgements

One of the authors (D.D.A) gratefully acknowledges the financial support received in the form of a research grant (Project No: 02-02-06-0101) and (Project No: 09-02-06-0057-SR005/09-07) from the Ministry of Science, Technology and Environment of Malaysia.

References

- [1] Han S, Martenak D J, Palermo R E *et al.* *J Catal*, 1994, **148**: 134
- [2] Han S, Kaufman E A, Martenak D J *et al.* *Catal Lett*, 1994, **29**: 27
- [3] Szoke A, Solymosi F. *Appl Catal A*, 1996, **142**: 361
- [4] Pierella L B, Wang L, Anunziata O A. *React Kinet Catal Lett*, 1997, **60**: 101
- [5] Weckhuysen B M, Wang D, Rosynek M P *et al.* *J Catal*, 1998, **175**: 338
- [6] Anggoro D D. [Master Thesis]. Malaysia: Universiti Teknologi Malaysia, 1998
- [7] Sharif Hussein S Z. [Master Thesis]. Malaysia: Universiti Teknologi Malaysia, 1999
- [8] Meriaudeau P, Ha V T T, Tiep L V. *Catal Lett*, 2000, **64**: 49
- [9] O'Connor C T, Kojima M. *Catal Today*, 1990, **6**: 329
- [10] Woolery G L, Kuehl G H, Timken H C *et al.* *Zeolites*, 1997, **19**: 288

- [11] Amin N A S, Anggoro D D. *J Natur Gas Chem*, 2002, **11**: 79
- [12] Pak S, Rades T, Rosynek M P et al. *Catal Lett*, 2000, **66**: 1
- [13] Hamid S A, Derouane E G, Demortier G et al. *Appl Catal A*, 1994, **108**: 85
- [14] Van Bekkum H, Flanigen E M, Jansen J C. *Stud Surf Sci Catal*, 1989, **58**: 233
- [15] Dyer A. An Introduction to Zeolite Molecular Sieves. New York: A Wiley-Interscience Publication, 1988. 34
- [16] Joseph George Post. [Ph.D Dissertation]. Nederland: Technische Hogeschool Eindhoven, 1984
- [17] Jansen J C, van der Gaag F J, van Bekkum H. *Zeolites*, 1984, **4**: 369
- [18] Le Van Mao R, Le T S, Fairbain M et al. *Appl Catal A*, 1999, **185**: 41
- [19] Szostak R. Molecular Sieves: Principles of Synthesis and Identifications. New York: Van Nostrand Reinhold, 1989. 26
- [20] Chu C T-W, Chang C D. *J Phys Chem*, 1985, **89**: 1569
- [21] Schuetze F W, Roessner F, Meusinger J et al. *Stud Surf Sci Catal*, 1997, **112**: 127
- [22] Sharifah Abdul Hamid. [Ph.D Dissertation]. Belgium: University of Namur, 1993
- [23] Fierro J L G. *Stud Surf Sci Catal*, 1990, **57**: A186
- [24] Loeffler E, Lohse U, Peuker Ch et al. *Zeolites*, 1990, **10**: 266
- [25] Oumi Y, Nemoto S, Nawata S et al. *Mater Chem Phys*, 2002, **78**: 551.
- [26] Woolery G L, Kuehl G H, Timken H C et al. *Zeolites*, 1997, **19**: 288
- [27] Hughes T R, White H M. *J Phys Chem*, 1967, **71**: 2192
- [28] Hedge S G, Kumar R, Bhat R N et al. *Zeolites*, 1989, **9**: 131
- [29] Borade R B, Clearfield A. *J Phys Chem*, 1992, **96**: 6729
- [30] Gnep N S, Doyement J Y, Guisnet M. *J Mol Catal*, 1988, **45**: 281
- [31] Guisnet M, Gnep N S, Vasques H et al. *Stud Surf Sci Catal*, 1991, **69**: 321
- [32] Parshall G W, Ittel S D. Homogeneous Catalysis. USA: A Wiley-Interscience Publication, 1992. 68
- [33] Choudhary V R, Panjala D, Banerjee S. *Appl Catal A*, 2002, **231**: 243
- [34] Nishi K, Komai S, Inagaki K et al. *Appl Catal A*, 2002, **223**: 187
- [35] Liu B, Yang Y, Sayari A. *Appl Catal A*, 2001, **214**: 95
- [36] Montes A, Giannetto G. *Appl Catal A*, 2000, **197**: 31
- [37] Protic-Lovasic G, Jambrec N, Deur-Siftar Prostenik M V. *Fuel*, 1990, **69**: 525